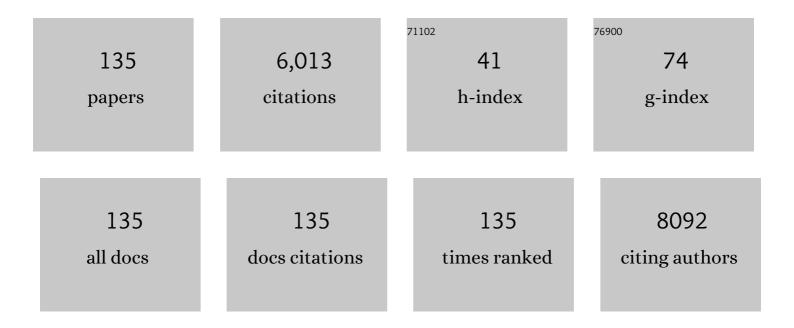
## Lars Thomsen

List of Publications by Year in descending order

Source: https://exaly.com/author-pdf/3705235/publications.pdf Version: 2024-02-01



#	Article	IF	CITATIONS
1	Critical Role of Alkyl Chain Branching of Organic Semiconductors in Enabling Solution-Processed N-Channel Organic Thin-Film Transistors with Mobility of up to 3.50 cm <sup>2</sup> V <sup>–1</sup> s <sup>–1</sup> . Journal of the American Chemical Society, 2013, 135, 2338-2349.	13.7	379
2	Macroscopic and high-throughput printing of aligned nanostructured polymer semiconductors for MHz large-area electronics. Nature Communications, 2015, 6, 8394.	12.8	280
3	A Quantitative Study of PCBM Diffusion during Annealing of P3HT:PCBM Blend Films. Macromolecules, 2009, 42, 8392-8397.	4.8	247
4	Direct insights into the role of epoxy groups on cobalt sites for acidic H2O2 production. Nature Communications, 2020, 11, 4181.	12.8	204
5	NEXAFS and XPS characterisation of carbon functional groups of fresh and aged biochars. Organic Geochemistry, 2014, 77, 1-10.	1.8	188
6	The Current Performance of the Wide Range (90–2500 eV) Soft X-ray Beamline at the Australian Synchrotron. AIP Conference Proceedings, 2010, , .	0.4	168
7	Iron Single Atoms on Graphene as Nonprecious Metal Catalysts for Highâ€Temperature Polymer Electrolyte Membrane Fuel Cells. Advanced Science, 2019, 6, 1802066.	11.2	164
8	Observation of a Distinct Surface Molecular Orientation in Films of a High Mobility Conjugated Polymer. Journal of the American Chemical Society, 2013, 135, 1092-1101.	13.7	150
9	Methods in carbon K-edge NEXAFS: Experiment and analysis. Journal of Electron Spectroscopy and Related Phenomena, 2006, 151, 105-120.	1.7	149
10	Chargeâ€Transport Anisotropy in a Uniaxially Aligned Diketopyrrolopyrroleâ€Based Copolymer. Advanced Materials, 2015, 27, 7356-7364.	21.0	144
11	A Long Cycleâ€Life Highâ€Voltage Spinel Lithiumâ€Ion Battery Electrode Achieved by Siteâ€Selective Doping. Angewandte Chemie - International Edition, 2020, 59, 10594-10602.	13.8	144
12	Vertical Stratification and Interfacial Structure in P3HT:PCBM Organic Solar Cells. Journal of Physical Chemistry C, 2010, 114, 15797-15805.	3.1	132
13	Performance, morphology and photophysics of high open-circuit voltage, low band gap all-polymer solar cells. Energy and Environmental Science, 2015, 8, 332-342.	30.8	115
14	Nanoscale Quantitative Chemical Mapping of Conjugated Polymer Blends. Nano Letters, 2006, 6, 1202-1206.	9.1	112
15	Chemically-synthesised, atomically-precise gold clusters deposited and activated on titania. Physical Chemistry Chemical Physics, 2013, 15, 3917.	2.8	111
16	<i>Quick AS NEXAFS Tool</i> ( <i>QANT</i> ): a program for NEXAFS loading and analysis developed at the Australian Synchrotron. Journal of Synchrotron Radiation, 2016, 23, 374-380.	2.4	110
17	Surface and Bulk Structural Characterization of a High-Mobility Electron-Transporting Polymer. Macromolecules, 2011, 44, 1530-1539.	4.8	105
18	Structure–Function Relationships of High-Electron Mobility Naphthalene Diimide Copolymers Prepared Via Direct Arylation. Chemistry of Materials, 2014, 26, 6233-6240.	6.7	105

#	Article	IF	CITATIONS
19	Microstructure of Polycrystalline PBTTT Films: Domain Mapping and Structure Formation. ACS Nano, 2012, 6, 1849-1864.	14.6	104
20	Highâ€Performance Allâ€Polymer Solar Cells Enabled by nâ€Type Polymers with an Ultranarrow Bandgap Down to 1.28 eV. Advanced Materials, 2020, 32, e2001476.	21.0	103
21	X-ray Microscopy of Photovoltaic Polyfluorene Blends:Â Relating Nanomorphology to Device Performance. Macromolecules, 2007, 40, 3263-3270.	4.8	102
22	Unraveling the Morphology of High Efficiency Polymer Solar Cells Based on the Donor Polymer PBDTTTâ€EFT. Advanced Energy Materials, 2015, 5, 1401259.	19.5	100
23	Alkylâ€Chainâ€Lengthâ€Independent Hole Mobility via Morphological Control with Poly(3â€alkylthiophene) Nanofibers. Advanced Functional Materials, 2010, 20, 792-802.	14.9	89
24	A multilayered approach to polyfluorene water-based organic photovoltaics. Solar Energy Materials and Solar Cells, 2012, 102, 114-124.	6.2	65
25	Tuning the Molecular Weight of the Electron Accepting Polymer in Allâ€Polymer Solar Cells: Impact on Morphology and Charge Generation. Advanced Functional Materials, 2018, 28, 1707185.	14.9	65
26	Nature and Extent of Solution Aggregation Determines the Performance of P(NDI2ODâ€T2) Thinâ€Film Transistors. Advanced Electronic Materials, 2018, 4, 1700559.	5.1	64
27	Photoreduction Kinetics of Sodium Tetrachloroaurate under Synchrotron Soft X-ray Exposure. Langmuir, 2011, 27, 8099-8104.	3.5	63
28	NEXAFS spectroscopy of conjugated polymers. European Polymer Journal, 2016, 81, 532-554.	5.4	63
29	Blade Coating Aligned, High-Performance, Semiconducting-Polymer Transistors. Chemistry of Materials, 2018, 30, 1924-1936.	6.7	63
30	Diamond Surfaces with Air‣table Negative Electron Affinity and Giant Electron Yield Enhancement. Advanced Functional Materials, 2013, 23, 5608-5614.	14.9	58
31	Unconventional Molecular Weight Dependence of Charge Transport in the High Mobility nâ€type Semiconducting Polymer P(NDI2ODâ€T2). Advanced Functional Materials, 2017, 27, 1604744.	14.9	58
32	X-ray Spectromicroscopy of Polymer/Fullerene Composites: Quantitative Chemical Mapping. Small, 2006, 2, 1432-1435.	10.0	57
33	Enhanced Electrochemical CO <sub>2</sub> Reduction of Cu@Cu <i><sub>x</sub></i> O Nanoparticles Decorated on 3D Vertical Graphene with Intrinsic sp <sup>3</sup> â€type Defect. Advanced Functional Materials, 2020, 30, 1910118.	14.9	54
34	Adsorption of organosilanes on iron and aluminium oxide surfaces. Surface and Interface Analysis, 1997, 25, 931-936.	1.8	53
35	Crystallographicâ€Siteâ€Specific Structural Engineering Enables Extraordinary Electrochemical Performance of Highâ€Voltage LiNi <sub>0.5</sub> Mn <sub>1.5</sub> O <sub>4</sub> Spinel Cathodes for Lithiumâ€Ion Batteries. Advanced Materials, 2021, 33, e2101413.	21.0	52
36	Structure Influence on Charge Transport in Naphthalenediimide–Thiophene Copolymers. Chemistry of Materials, 2014, 26, 6796-6804.	6.7	51

#	Article	IF	CITATIONS
37	One-Step Method for Generating PEG-Like Plasma Polymer Gradients: Chemical Characterization and Analysis of Protein Interactions. Langmuir, 2010, 26, 13987-13994.	3.5	48
38	Evolution of the nanomorphology of photovoltaic polyfluorene blends: sub-100 nm resolution with x-ray spectromicroscopy. Nanotechnology, 2008, 19, 424015.	2.6	47
39	The adsorption and stability of sulfur containing amino acids on Cu{531}. Surface Science, 2009, 603, 1253-1261.	1.9	44
40	Evolution of Laterally Phase-Separated Polyfluorene Blend Morphology Studied by X-ray Spectromicroscopy. Macromolecules, 2009, 42, 3347-3352.	4.8	43
41	Influence of Fluorination and Molecular Weight on the Morphology and Performance of PTB7:PC <sub>71</sub> BM Solar Cells. Journal of Physical Chemistry C, 2014, 118, 9918-9929.	3.1	43
42	Electrochemically substituted metal phthalocyanines, e-MPc (M = Co, Ni), as highly active and selective catalysts for CO <sub>2</sub> reduction. Journal of Materials Chemistry A, 2018, 6, 1370-1375.	10.3	43
43	Role of Solvent Trapping Effects in Determining the Structure and Morphology of Ternary Blend Organic Devices. Macromolecules, 2009, 42, 3098-3103.	4.8	42
44	Valence Alignment of Mixed Ni–Fe Hydroxide Electrocatalysts through Preferential Templating on Graphene Edges for Enhanced Oxygen Evolution. ACS Nano, 2020, 14, 11327-11340.	14.6	42
45	Critical Role of Pendant Group Substitution on the Performance of Efficient All-Polymer Solar Cells. Chemistry of Materials, 2017, 29, 804-816.	6.7	41
46	Self-Assembly of ABC Bottlebrush Triblock Terpolymers with Evidence for Looped Backbone Conformations. Macromolecules, 2018, 51, 7178-7185.	4.8	40
47	A facile approach to alleviate photochemical degradation in high efficiency polymer solar cells. Journal of Materials Chemistry A, 2015, 3, 16313-16319.	10.3	38
48	Influence of Fullerene Acceptor on the Performance, Microstructure, and Photophysics of Low Bandgap Polymer Solar Cells. Advanced Energy Materials, 2017, 7, 1602197.	19.5	38
49	XPS and NEXAFS study of fluorine modified TiO2 nano-ovoids reveals dependence of Ti3+ surface population on the modifying agent. RSC Advances, 2014, 4, 20649.	3.6	37
50	A template-free method to synthesis high density iron single atoms anchored on carbon nanotubes for high temperature polymer electrolyte membrane fuel cells. Nano Energy, 2021, 80, 105534.	16.0	35
51	Probing the nature of soil organic matter. Critical Reviews in Environmental Science and Technology, 2022, 52, 4072-4093.	12.8	35
52	Extremely high negative electron affinity of diamond via magnesium adsorption. Physical Review B, 2015, 92, .	3.2	34
53	Influence of alkyl side-chain type and length on the thin film microstructure and OFET performance of naphthalene diimide-based organic semiconductors. Organic Electronics, 2019, 75, 105378.	2.6	33
54	Influence of Cationic Surfactants on the Formation and Surface Oxidation States of Gold Nanoparticles Produced via Laser Ablation. Langmuir, 2013, 29, 12452-12462.	3.5	32

#	Article	IF	CITATIONS
55	Tuning the Electrochemical Property of the Ultrafine Metalâ€oxide Nanoclusters by Iron Phthalocyanine as Efficient Catalysts for Energy Storage and Conversion. Energy and Environmental Materials, 2019, 2, 5-17.	12.8	32
56	Investigating the order–disorder phase transition in Nd2â^'xYxZr2O7via diffraction and spectroscopy. Dalton Transactions, 2013, 42, 14875.	3.3	31
57	Isolating and quantifying the impact of domain purity on the performance of bulk heterojunction solar cells. Energy and Environmental Science, 2017, 10, 1843-1853.	30.8	31
58	Impact of Acceptor Fluorination on the Performance of All-Polymer Solar Cells. ACS Applied Materials & Interfaces, 2018, 10, 955-969.	8.0	31
59	Unravelling donor–acceptor film morphology formation for environmentally-friendly OPV ink formulations. Green Chemistry, 2019, 21, 5090-5103.	9.0	31
60	Photoelectron emission from lithiated diamond. Physica Status Solidi (A) Applications and Materials Science, 2014, 211, 2209-2222.	1.8	30
61	Single Crystal X-ray, AFM, NEXAFS, and OFET Studies on Angular Polycyclic Aromatic Silyl-Capped 7,14-Bis(ethynyl)dibenzo[b,def]chrysenes. Crystal Growth and Design, 2012, 12, 725-731.	3.0	29
62	First demonstration of phosphate enhanced atomically dispersed bimetallic FeCu catalysts as Pt-free cathodes for high temperature phosphoric acid doped polybenzimidazole fuel cells. Applied Catalysis B: Environmental, 2021, 284, 119717.	20.2	28
63	Near-edge X-ray absorption fine-structure spectroscopy of naphthalene diimide-thiophene co-polymers. Journal of Chemical Physics, 2014, 140, 164710.	3.0	27
64	Introducing 4 <i>s</i> –2 <i>p</i> Orbital Hybridization to Stabilize Spinel Oxide Cathodes for Lithiumâ€ion Batteries. Angewandte Chemie - International Edition, 2022, 61, .	13.8	26
65	Understanding the Conformational Dynamics of Organosilanes: γ-APS on Zinc Oxide Surfaces. Langmuir, 2002, 18, 148-154.	3.5	25
66	A study of the initial film growth of PEG-like plasma polymer films via XPS and NEXAFS. Applied Surface Science, 2014, 288, 288-294.	6.1	24
67	Molecular nitrogen acceptors in ZnO nanowires induced by nitrogen plasma annealing. Physical Review B, 2015, 92, .	3.2	24
68	Impact of Fullerene Mixing Behavior on the Microstructure, Photophysics, and Device Performance of Polymer/Fullerene Solar Cells. ACS Applied Materials & Interfaces, 2016, 8, 29608-29618.	8.0	24
69	Coulomb Enhanced Charge Transport in Semicrystalline Polymer Semiconductors. Advanced Functional Materials, 2016, 26, 8011-8022.	14.9	24
70	Insight into thin-film stacking modes of π-expanded quinoidal molecules on charge transport property via side-chain engineering. Journal of Materials Chemistry C, 2017, 5, 1935-1943.	5.5	24
71	Critical Role of Molecular Symmetry for Charge Transport Properties: A Paradigm Learned from Quinoidal Bithieno[3,4- <i>b</i> ]thiophenes. Chemistry of Materials, 2017, 29, 4999-5008.	6.7	24
72	Reconstructing Cu Nanoparticle Supported on Vertical Graphene Surfaces via Electrochemical Treatment to Tune the Selectivity of CO <sub>2</sub> Reduction toward Valuable Products. ACS Catalysis, 2022, 12, 4792-4805.	11.2	24

#	Article	IF	CITATIONS
73	New Insights into the Substrate–Plasma Polymer Interface. Journal of Physical Chemistry B, 2011, 115, 6495-6502.	2.6	23
74	Morphological and Device Evaluation of an Amphiphilic Block Copolymer for Organic Photovoltaic Applications. Macromolecules, 2017, 50, 4942-4951.	4.8	22
75	Highly Selective Metalâ€Free Electrochemical Production of Hydrogen Peroxide on Functionalized Vertical Graphene Edges. Small, 2022, 18, e2105082.	10.0	20
76	A NEXAFS orientation study of $\hat{1}^3$ -aminopropyltriethoxysilane on zinc oxide surfaces. Surface and Interface Analysis, 2006, 38, 1139-1145.	1.8	19
77	Highly resilient field emission from aligned single-walled carbon nanotube arrays chemically attached to n-type silicon. Journal of Materials Chemistry, 2008, 18, 5753.	6.7	19
78	Investigating the Enantioselectivity of Alanine on a Chiral Cu{421} <sup>R</sup> Surface. Journal of Physical Chemistry C, 2012, 116, 9472-9480.	3.1	19
79	NEXAFS spectroscopy of CVD diamond films exposed to fusion relevant hydrogen plasma. Diamond and Related Materials, 2013, 34, 45-49.	3.9	19
80	Resonant Tender X-ray Diffraction for Disclosing the Molecular Packing of Paracrystalline Conjugated Polymer Films. Journal of the American Chemical Society, 2021, 143, 1409-1415.	13.7	19
81	Retention and damage in 3C-β SiC irradiated with He and H ions. Journal of Nuclear Materials, 2016, 469, 187-193.	2.7	18
82	The impact of tetrahedral capping groups and device processing conditions on the crystal packing, thin film features and OFET hole mobility of 7,14-bis(ethynyl)dibenzo[b,def]chrysenes. Journal of Materials Chemistry C, 2013, 1, 6299.	5.5	17
83	On the Relation between Morphology and FET Mobility of Poly(3â€alkylthiophene)s at the Polymer/SiO <sub>2</sub> and Polymer/Air Interface. Advanced Functional Materials, 2014, 24, 1994-2004.	14.9	17
84	Lyotropic Liquid Crystalline Mesophase Governs Interfacial Molecular Orientation of Conjugated Polymer Thin Films. Chemistry of Materials, 2020, 32, 6043-6054.	6.7	17
85	Thionation of naphthalene diimide molecules: Thin-film microstructure and transistor performance. Organic Electronics, 2018, 53, 287-295.	2.6	16
86	Adsorption and orientation kinetics of self-assembled films of octadecyltrimethoxysilane on aluminium oxide surfaces. Surface and Interface Analysis, 2005, 37, 472-477.	1.8	15
87	Arbuscular mycorrhizal symbiosis enhances water stable aggregate formation and organic matter stabilization in Fe ore tailings. Geoderma, 2022, 406, 115528.	5.1	15
88	Sculpting nanoscale precipitation patterns in nanocomposite thin films via hyperthermal ion deposition. Applied Physics Letters, 2010, 97, .	3.3	14
89	High performance as-cast P3HT:PCBM devices: understanding the role of molecular weight in high regioregularity P3HT. Materials Advances, 2021, 2, 2045-2054.	5.4	14
90	Metal Evaporation-Induced Degradation of Fullerene Acceptors in Polymer/Fullerene Solar Cells. ACS Applied Materials & Interfaces, 2016, 8, 2247-2254.	8.0	13

#	Article	IF	CITATIONS
91	Introducing 4 <i>s</i> –2 <i>p</i> Orbital Hybridization to Stabilize Spinel Oxide Cathodes for Lithiumâ€Ion Batteries. Angewandte Chemie, 2022, 134, .	2.0	12
92	Determining the Electronic Confinement of a Subsurface Metallic State. ACS Nano, 2014, 8, 10223-10228.	14.6	11
93	Dissociation of CH <sub>3</sub> –O as a Driving Force for Methoxyacetophenone Adsorption on Si(001). Journal of Physical Chemistry C, 2019, 123, 22239-22249.	3.1	11
94	Surface reactions between CO2 and H over K-modified Cu(001). Vacuum, 2006, 81, 25-31.	3.5	10
95	p-f hybridization in the ferromagnetic semiconductor HoN. Applied Physics Letters, 2012, 100, 072108.	3.3	10
96	Manipulating the orientation of an organic adsorbate on silicon: a NEXAFS study of acetophenone on Si(0 0 1). Journal of Physics Condensed Matter, 2015, 27, 054002.	1.8	10
97	The Structural Origin of Electron Injection Enhancements with Fulleropyrrolidine Interlayers. Advanced Materials Interfaces, 2016, 3, 1500852.	3.7	10
98	Diamond structure recovery during ion irradiation at elevated temperatures. Nuclear Instruments & Methods in Physics Research B, 2015, 365, 331-335.	1.4	9
99	A simple polarimeter for quantifying synchrotron polarization. Journal of Electron Spectroscopy and Related Phenomena, 2006, 151, 208-214.	1.7	8
100	Enantiospecific Adsorption and Decomposition of Cysteine Enantiomers on the Chiral Cu{421} <sup>R</sup> Surface. Journal of Physical Chemistry C, 2019, 123, 20829-20837.	3.1	8
101	Fluorescence and Physico-Chemical Properties of Hydrogenated Detonation Nanodiamonds. Journal of Carbon Research, 2020, 6, 7.	2.7	8
102	Morphology and Charge Transport Properties of P(NDI2OD-T2)/Polystyrene Blends. Macromolecules, 2021, 54, 11134-11146.	4.8	8
103	Adsorption of hydrogen on clean and potassium modified low index copper surfaces: Cu(100) and Cu(110). Journal of Vacuum Science and Technology A: Vacuum, Surfaces and Films, 2001, 19, 1988-1992.	2.1	7
104	An unconventional method for measuring the Tc <i>L</i> <sub>3</sub> -edge of technetium compounds. Journal of Synchrotron Radiation, 2014, 21, 1275-1281.	2.4	7
105	Boron coordination structure at the surfaces of sodium borosilicate and aluminoborosilicate glasses by B K-edge NEXAFS. Journal of Non-Crystalline Solids, 2020, 545, 120247.	3.1	7
106	Deuterium retention and near-surface modification of ion-irradiated diamond exposed to fusion-relevant plasma. Nuclear Fusion, 2014, 54, 073003.	3.5	6
107	D and D/He plasma interactions with diamond: Surface modification and D retention. Diamond and Related Materials, 2014, 49, 103-110.	3.9	6
108	Adsorption differences between low coverage enantiomers of alanine on the chiral Cu{421} <sup>R</sup> surface. Physical Chemistry Chemical Physics, 2017, 19, 13562-13570.	2.8	6

#	Article	IF	CITATIONS
109	Determining the Orientation of a Chiral Substrate Using Full-Hemisphere Angle-Resolved Photoelectron Spectroscopy. Physical Review Letters, 2011, 107, 175501.	7.8	5
110	Measurement of molecular order and orientation in nanoscale organic films. Synthetic Metals, 2005, 152, 21-24.	3.9	4
111	Photoabsorption and photoemission of magnesium diboride at the Mg K edge. Journal of Physics Condensed Matter, 2009, 21, 405701.	1.8	4
112	Direct observation of phonon emission from hot electrons: spectral features in diamond secondary electron emission. Journal of Physics Condensed Matter, 2014, 26, 395008.	1.8	4
113	Ion irradiated graphite exposed to fusion-relevant deuterium plasma. Nuclear Instruments & Methods in Physics Research B, 2014, 340, 21-26.	1.4	4
114	The templated growth of a chiral transition metal chalcogenide. Surface Science, 2014, 629, 94-101.	1.9	4
115	Orientation and stability of a bi-functional aromatic organic molecular adsorbate on silicon. Physical Chemistry Chemical Physics, 2016, 18, 27290-27299.	2.8	4
116	Effect of Thionation on the Performance of PNDIT2-Based Polymer Solar Cells. Journal of Physical Chemistry C, 2019, 123, 12062-12072.	3.1	4
117	Impact of Polymer Molecular Weight on Polymeric Photodiodes. Advanced Optical Materials, 2022, 10, 2101890.	7.3	4
118	NEXAFS microscopy of polymeric materials: Successes and challenges encountered when characterizing organic devices. Journal of Physics: Conference Series, 2009, 186, 012102.	0.4	3
119	Field ionization detectors: a comparative model. Measurement Science and Technology, 2011, 22, 015901.	2.6	3
120	A step towards long-wavelength protein crystallography: subjecting protein crystals to a vacuum. Journal of Applied Crystallography, 2015, 48, 913-916.	4.5	3
121	Thermal migration of alloying agents in aluminium. Materials Research Express, 2016, 3, 116501.	1.6	3
122	Self-Assembly of ABC Bottlebrush Triblock Terpolymers with Evidence for Looped Backbone Conformations. Macromolecules, 2018, 51, .	4.8	3
123	Resolving the backbone tilt of crystalline poly(3-hexylthiophene) with resonant tender X-ray diffraction. Materials Horizons, 2022, 9, 1649-1657.	12.2	3
124	Reassessing the Significance of Reduced Aggregation and Crystallinity of Naphthalene Diimide-Based Copolymer Acceptors in All-Polymer Solar Cells. ACS Applied Polymer Materials, 2022, 4, 3270-3282.	4.4	3
125	Measuring the Tilt Angle of ODTMS Self-Assembled Monolayers on Al Oxide Surfaces. Synthetic Metals, 2005, 154, 9-12.	3.9	2
126	Adsorption and Dissociation of a Bicyclic Tertiary Diamine, Triethylenediamine, on a Si(100)-2 × 1 Surface. Journal of Physical Chemistry C, 2016, 120, 28672-28681.	3.1	2

#	Article	IF	CITATIONS
127	Robustp-type doping of copper oxide using nitrogen implantation. Materials Research Express, 2017, 4, 075905.	1.6	2
128	Accelerated ageing of molybdenum oxide. Materials Research Express, 2017, 4, 115502.	1.6	2
129	Chain Alignment and Charge Transport Anisotropy in Blade-Coated P(NDI2OD-T2)/PS Blend Films. ACS Applied Polymer Materials, 2022, 4, 5501-5514.	4.4	2
130	Determining the angular admittance of a cylindrical mirror analyser. Surface and Interface Analysis, 2002, 34, 782-785.	1.8	0
131	Towards fabrication of synthetic metal nanowires. Synthetic Metals, 2005, 154, 33-36.	3.9	0
132	Rapid Deposition of LDS/Carbon Nanotube Composites: A Novel Nanotube Field Emission Source. , 2006, , .		0
133	PTMS alignment on Aluminium Oxide. , 2006, , .		0
134	A simple method for creating nanotube field emitters from a surfactant dispersion. Surface Science, 2007, 601, 5775-5778.	1.9	0
135	Electronic States Studies of ZnOâ^•TiO[sub 2] Core-Shell Nanostructure by Photoelectron Spectroscopy and X-Ray Absorption Near Edge Spectroscopy. , 2010, , .		Ο